Temporally and spatially coordinated roles for Rho, Rac, Cdc42 and their effectors in growth cone guidance by a physiological electric field

Ann M. Rajnicek*, Louise E. Foubister and Colin D. McCaig

School of Medical Sciences, Institute of Medical Sciences, University of Aberdeen, Aberdeen, Scotland, AB25 2ZD, UK

*Author for correspondence (e-mail: a.m.rajnicek@abdn.ac.uk)

Accepted 19 January 2006
Journal of Cell Science 119, 1723-1735 Published by The Company of Biologists 2006
doi:10.1242/jcs.02896

Summary

Although it is known that neuronal growth cones migrate towards the cathode of an applied direct current (DC) electric field (EF), resembling the EF present in the developing nervous system, the underlying mechanism remains unclear. Here, we demonstrate temporally and spatially coordinated roles for the GTPases Rac, Cdc42 and Rho and their effectors. Growth cones of cultured *Xenopus* embryonic spinal neurons turned towards the cathode but collective inhibition of Rho, Rac and Cdc42 attenuated turning. Selective inhibition of Rho, Cdc42 or Rac signalling revealed temporally distinct roles in steering by an electrical gradient. Rho, Rac and Cdc42 are each essential for turning within the initial 2 hours (early phase). Later, Rho and Cdc42 signals remain important but Rac signalling dominates. The EF increased Rho immunofluorescence anodally. This correlated spatially with collapsed growth cone morphology and reduced anodal migration rates, which were restored by Rho inhibition. These data suggest that anodally increased Rho activity induces local cytoskeletal collapse, biasing growth cone advance cathodally. Collapse might be mediated by the Rho effectors p160 Rho kinase and myosin light chain kinase since their inhibition attenuated early turning. Inhibitors of phosphoinositide 3-kinase, MEK1/2 or p38 mitogen-activated protein kinase (MAPK) did not affect turning behaviour, eliminating them mechanistically. We propose a mechanism whereby Rac and Cdc42 activities dominate cathodally and Rho activity dominates anodally to steer growth cones towards the cathode. The interaction between Rho GTPases, the cytoskeleton and growth cone dynamics is explored in the companion paper published in this issue. Our results complement studies of growth cone guidance by diffusible chemical gradients and suggest that growth cones might interpret these co-existing guidance cues selectively.

Key words: Axon guidance, Electric field, Rho GTPases

Introduction

Nervous system function requires 'hard-wired' circuits resulting from the extension of neuronal processes (neurites) over long distances to specific targets. Growth cones, the tips of extending neurites, are guided in embryos and during regeneration by extracellular cues including gradients of chemoattractive and chemorepulsive molecules (Yamamoto, 2002). Steady, direct current (DC) electric fields (EFs) co-exist with these molecular gradients for prolonged periods (Hotary and Robinson, 1991; Shi and Borgens, 1995) (reviewed by McCaig et al., 2002; McCaig et al., 2005). The basis for the EF is the transepithelial potential (TEP) across the intact epithelium. In *Xenopus* embryos, a TEP of approximately +60 mV (inside positive) is generated by the inward movement of Na^+ ions across the skin. In regions where epithelial integrity is disturbed, for example by breakdown of tight junctions prior to cell migration, the TEP collapses locally but remains intact distally. This generates a voltage gradient (EF) within the tissues beneath (parallel to) the epithelium. The neural tube, the precursor of the brain and spinal cord, shares an ectodermal origin with skin and generates its own TEP such that the entire nervous system develops within a natural EF of hundreds of mV/mm (Hotary and Robinson, 1991; Shi and Borgens, 1994; Shi and Borgens, 1995). The EF varies developmentally and spatially, and is highest across developmentally key regions, such as the floor plate (McCaig et al., 2005).

EFs are usually omitted from the list of recognised growth cone guidance cues despite evidence that disruption of naturally occurring EFs perturbs normal nervous system development (Hotary and Robinson, 1992; Hotary and Robinson, 1994; Metcalf and Borgens, 1994), successful completion of a Phase I clinical trial in which a DC EF was applied to neurologically complete human spinal cord injuries (Shapiro et al., 2005), and evidence that EFs direct neurite growth in vivo (Song et al., 2004) and in vitro (Hinkle et al., 1981; McCaig, 1987; Rajnicek et al., 1998). Neurites of dissociated, embryonic, *Xenopus* spinal neurons grow faster towards the negative pole of the EF (cathode), retract from the positive pole (anode) and branch more often towards the cathode, and growth cones turn to migrate towards the cathode. Cathodally directed growth occurs in an EF as small as 7 mV/mm (Hinkle et al., 1981), which is at least 50 times smaller than the EFs that developing neurons encounter naturally in vivo. Significantly, regenerating mammalian nerves in vivo

Journal of Cell Science

Journal of Cell Science

respond with similar cathodally directed growth, turning and branching in a naturally occurring EF of about 40 mV/mm (Song et al., 2004; Sta Iglesia and Vanable, Jr, 1998).

Assuming a threshold EF strength of 10 mV/mm, the voltage gradient across a 10 μm wide growth cone is 0.1 mV. The mechanism by which a growth cone senses this small gradient and translates it into a directional response remains unclear but several parallels exist with growth cone chemotropism, in which growth cones detect and amplify (through spatially regulated signal transduction) shallow chemical gradients (McCaig et al., 2005). Mechanistically, both require signalling through cytoplasmic Ca^{2+}, phospholipase C (PLC), and activation of receptors for neurotrophin-3 (NT-3), brain-derived growth factor (BDNF), acetylcholine (ACh) and fibroblast growth factor (FGF). EF guidance is presumed to involve EF-induced asymmetric localisation or activation of channels or receptors in the plasma membrane (reviewed by McCaig et al., 2002; McCaig et al., 2005), particularly voltage-gated Ca^{2+} channels (Stewart et al., 1995) and receptors for ACh, NT-3 and BDNF (Fig. 7A). How asymmetric activation of these molecules steers growth cones towards the cathode has not been established but any proposal must link these molecules to spatial regulation of the cytoskeleton.

A probable link between the candidate molecules and the cytoskeleton is the Rho family of small GTPases, which includes Rac, Rho and Cdc42. These molecules are downstream of activation of the candidate membrane receptors (and Ca^{2+} signals), upstream of effectors of cytoskeletal dynamics, and are proposed to mediate directional migration of growth cones (Jin et al., 2005; Mueller, 1999) and other cells in chemical gradients (Fukata et al., 2003; Kaibuchi et al., 1999). Genetic disruption of GTPase activity induces growth cone path-finding defects in embryos (Kaufmann et al., 1998; Kim et al., 2002), suggesting that precise spatiotemporal regulation of Rho GTPases is crucial for normal growth cone guidance.

According to the predominant model, growth cone chemoattraction results from activation of Cdc42 and Rac on the side of the growth cone facing the attractant (and consequent inhibition of Rho), whereas chemorepulsion is mediated by activation of Rho on the side facing the repellent (and inhibition of Rac and Cdc42) (Mueller, 1999; Song and Poo, 2001; Patel and Van Vactor, 2002). Activation of Cdc42 and Rac stimulates growth cone filopodia and lamellipodia, respectively, whereas RhoA activation stimulates contraction of the actin cytoskeleton leading to growth cone collapse (Kozma et al., 1997; Kim et al., 2002; Yuan et al., 2003).

The aim of the present study was to explore the role of the small GTPases Rac, Cdc42 and Rho and their effectors in EF-induced growth cone steering. The mechanistic link between signalling by the small GTPases, the cytoskeleton and growth cone dynamics in an EF are explored in the companion paper in this issue (Rajnicek et al., 2006). Here, we show that Rac, Cdc42 and Rho are each involved in guidance of growth cones by EFs and that Rac signalling predominates during the late phase (>2 hours) of EF exposure. Turning during the early phase (<2 hours) requires activity of the Rho GTPase effectors myosin light chain kinase (MLCK), citron kinase (citron-K), rhotekin-rhophilin-protein kinase N (PKN) and p160 Rho kinase (p160 ROCK). By contrast, cathodal turning does not require phosphoinositide 3-kinase (PI 3-kinase), p38 mitogen-activated protein kinase (MAPK) or extracellular signal related kinase (ERK1/2) activity, which have been implicated previously in EF guidance of non-neuronal cells (Zhao et al., 2002) and chemoattraction of growth cones (Campbell and Holt, 2003). These data suggest mechanistic differences between steering in chemical and electrical gradients. A model for the intracellular cascades involved in EF guidance of growth cones is presented.

It is particularly important to elucidate the mechanisms that underpin EF influences on neuronal growth and guidance in light of a recently completed clinical trial testing the ability of a DC EF to stimulate human spinal cord regeneration (Shapiro et al., 2005). Since Rho is activated following spinal cord injury (Madura et al., 2004) and Rho inhibition improves adult mammalian spinal cord repair (Fourneir et al., 2003; Sung et al., 2003), an understanding of the interaction between Rho GTPases and EF-induced growth cone guidance would suggest novel combinations of electrical/pharmacological therapies.

Results

Neuronal growth cones migrate directionally towards the cathode

Consistent with previous studies (e.g. Hinkle et al., 1981; Patel and Poo, 1982; Rajnicek et al., 1998), *Xenopus* spinal neurons without an EF exhibited randomly oriented neurite extension whereas those exposed to an EF of 150 mV/mm for 5 hours reoriented strikingly towards the cathode (Fig. 1A-D). Without an EF, growth cones turned +3±6° and migrated at 19.6±2.1 μm/hour; in an EF, growth cones migrated faster (31.4±2.3 μm/hour) and turned –53±5° towards the cathode (expect 0° if random; negative values indicate net cathodal turning, positive values indicate net anodal turning). The EF also increased the frequency of cathodal turning; 76% (65/85) turned towards the cathode, and decreased the frequency of anodal turning to 8% (7/85) compared with no EF controls in which 27% (13/49) of growth cones turned towards the cathode and 39% (19/49) turned towards the anode. The controls are indistinguishable from the theoretical frequency of 33% for random growth.

Control experiments (drug, no EF) were performed for all pharmacological treatments in Figs 1-6 (data not shown). Neurite extension was random (not different from the 'without EF' data above). The mean angle turned during 5 hours ranged from –6±8° in Rho 23-40 (n=49) to +8±6° in 10 ng/ml toxin B (TxB) (n=40).

Rho GTPases are involved in cathodal growth cone guidance

The Rho family of small GTPases has been implicated in chemoattractive turning of *Xenopus* growth cones (Yuan et al., 2003; Mueller, 1999). We used the same pharmacological inhibitors of Rho GTPases and their effectors from those studies to explore the mechanism for cathodal turning. The broad-spectrum Rho GTPase inhibitor TxB derived from *Clostridium difficile* inhibits RhoA, Rac 1 and Cdc42 collectively (Chavez-Olarte et al., 1997) and attenuated turning in 0.01 ng/ml or 10 ng/ml (Fig. 1A,B,D). The mean angle turned during 5 hours of EF exposure (Fig. 1A) and the frequency of cathodal turning (Fig. 1B) were reduced compared with EF-treated growth cones in the absence of any inhibitor, but the frequency of anodal turning was not affected by TxB (Fig. 1B). Similar cathodal attenuation was observed

in 0.1 ng/ml TxB (n=50, data not shown). The diminished turning response in TxB was not a result of failure of neurite extension since growth cone migration rates exceeded (in 0.01 ng/ml) or were identical to (in 0.1 ng/ml or 10 ng/ml) those without the drug (Fig. 1C). These data implicate Rac, Cdc42 and Rho collectively in cathodal orientation but do not allow discrimination of the selective requirements of Rac, Rho or Cdc42.

Cdc42 and Rac mediate cathodal turning

We dissected the involvement of individual family members in EF guidance using custom-synthesised peptides that perturb Rac or Cdc42 signalling selectively (Vastrik et al., 1999) and C3 transferase (from *Clostridium botulinum*, also known as C3 exoenzyme) to inhibit RhoA (Aktories et al., 1989; Narumiya et al., 1990). The synthetic peptides correspond to amino acids 17-32 on the N-terminus of Rac 1 (Rac 17-32) or Cdc42 (Cdc42 17-32) and are each tagged with a TAT internalisation sequence on the C-terminus. The peptides correspond to the CRIB (Cdc42/Rac-1 binding) domain on Rac or Cdc42. These peptides were selected because, from an overlapping series of peptides, only Rac 17-32 but not Cdc42 17-32 or Rho 17-32 inhibited collapse of dorsal root ganglion growth cones (Vastrik et al., 1999), demonstrating peptide specificity on growth cone behaviour. In addition, Rac 17-32 or Cdc42 17-32 each prevented retraction of axons upon contact with a repulsive cue (Thies and Davenport, 2002), suggesting a role in neurite guidance. The peptides compete with activated Rac or Cdc42 for binding to effector proteins and therefore prevent signalling downstream (Vastrik et al., 1999). Peptides were added to the cultures at least 1 hour prior to EF exposure and remained in the medium throughout the experiment.

In 10 μg/ml Rac 17-32, growth cones migrated randomly during the entire 5 hours of EF exposure (Fig. 2). The mean angle turned (Fig. 2A) and the frequencies of cathodal and anodal turning (Fig. 2B) were the same as for growth cones without an EF. Therefore, inhibition of Rac signalling abolished cathodal orientation throughout the entire 5 hours.

The effect of Cdc42 17-32 on growth cone turning was biphasic. In 10 μg/ml Cdc42 17-32, growth cones did not turn at all during the first 2 hours of EF exposure (–0.3±2°) and, by 5 hours, had turned only –13±4 deg (n=177). Therefore, cathodal turning was abolished by Cdc42 17-32 in the first 2 hours and cathodal turning at 5 hours was attenuated substantially (P<0.0001 compared with EF alone) but not abolished (P=0.0274 compared with no EF) (Fig. 2A,D). A similar trend was observed for the frequency of cathodal turning (Fig. 2B). The frequency turning at 2 hours (27%, 48/177) was reduced (P<0.001) compared with 72% (61/85) without the peptide. By 5 hours, only 40% (71/177) had turned cathodally, significantly less than without the peptide (76%, 65/85, P<0.001) (Fig. 2B). Although it attenuated cathodal turning, Cdc42 17-32 did not abolish turning at 5 hours, as Rac 17-32 had done (Fig. 2A). The peptides also differ in their effect on neurite outgrowth. Growth cones migrated more rapidly in Rac 17-32 than in Cdc42 17-32 (Fig. 2C). Since the peptides differ by only two amino acids and contain identical TAT sequences, the differences in growth cone behaviour suggest different functional specificities and reduce significantly the possibility that the TAT sequence itself causes the inhibitory effects. Moreover, growth cone morphology differed in the two peptides (Rajnicek et al., 2006) in a manner consistent with selective inhibition of either Rac or Cdc42,

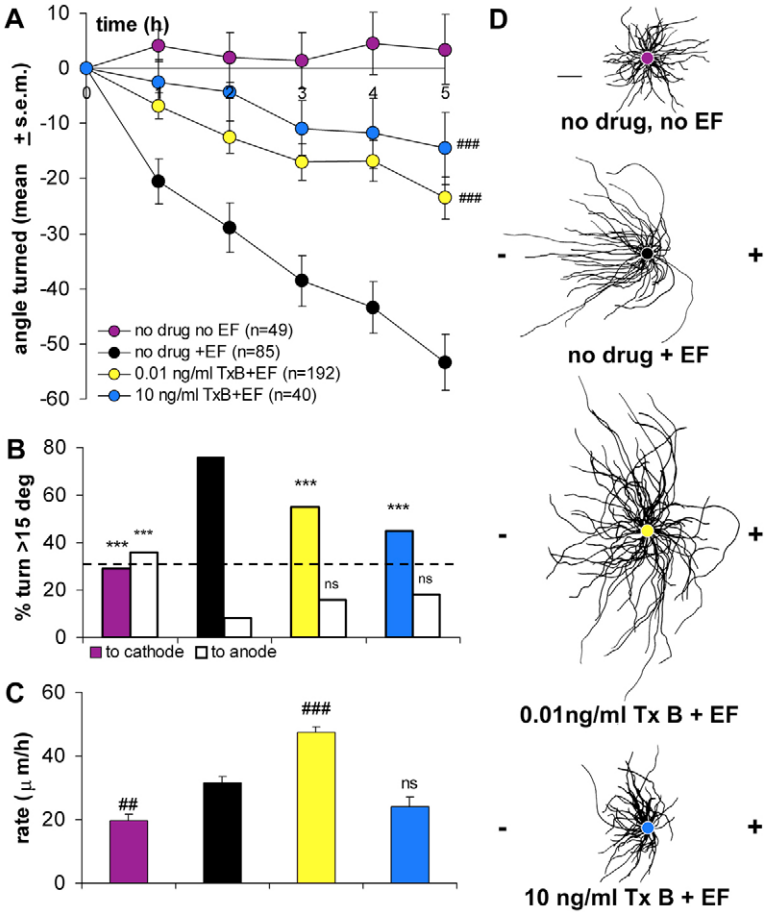

Fig. 1. Collective inhibition of Rac, Rho and Cdc42 with toxin B attenuates cathodal growth cone steering by an EF. (A) Mean angle turned by growth cones during 5 hours. In the absence of an EF, growth cones migrate randomly (mean angle turned would be 0° for random migration) but, in an EF of 150 mV/mm, growth cones turn towards the cathode. Negative values indicate net cathodal deflection. The number of growth cones measured is in parentheses. The mean angle turned at 5 hours was compared with 'no drug + EF' using a Student's two-tailed t test; TxB, toxin B; $^{###}P$<0.0001. (B) Percentage of growth cones (see A for total) that turn towards the cathode (filled bars) or anode (open bars) in 5 hours. The dotted line is the expected frequency for random orientation (33%). Asterisks compare cathodal or anodal frequencies with no drug + EF; ***P<0.001. (C) Mean rate of growth cone advance during 5 hours of EF exposure compared with no drug + EF (black bar) using a two-tailed Student's t test. $^{##}P$=0.002; $^{###}P$<0.0001. See A for number of growth cones. (D) Composite drawings made from images of individual, dissociated neurons at the end of a 5-hour experiment. Somas were superimposed at the coloured dot and the path of each neurite was traced. The EF vector is horizontal, with cathode at left and anode at right. Bar, 100 μm for all drawings. ns, not significant.

Journal of Cell Science

again suggesting specificity of the compounds in the presence of identical TAT sequences. Filopodia were retained but lamellipodia were reduced significantly in Rac 17-32. Conversely, growth cones in Cdc42 17-32 had few filopodia but well developed lamellipodia.

Disrupting Rho signalling inhibits cathodal turning

RhoA involvement in cathodal turning was tested using C3 transferase, which ADP-ribosylates RhoA in the effector domain, therefore preventing interaction with effectors (Aktories et al., 1989; Narumiya et al., 1990). Cathodal turning at 5 hours was attenuated by 1 μg/ml or 20 μg/ml (Fig. 2). The turning response in 20 μg/ml C3 transferase was quantitatively and temporally similar to that in Cdc42 17-32, with no turning within the first 2 hours, severely attenuated turning between 2 and 5 hours (Fig. 2A) and fewer growth cones turning cathodally by 5 hours than without the drug (Fig. 2B). Cathodal turning was attenuated throughout the entire 5 hours in 1 μg/ml C3 transferase but less than in 20 μg/ml (Fig. 2A). The frequency of cathodal turning was also decreased in 20 μg/ml (Fig. 2B). Attenuated turning in 20 μg/ml was not attributable to poor growth cone advance because, although the migration rate was reduced compared with EF-treated cells without an inhibitor, it was the same as for growth cones without any drug or EF (Fig. 2C).

In non-neuronal cells, L-α-lysophosphatidic acid (LPA) induces Rho activation through the LPA receptor-PDZ-RhoGEF complex (Yamada et al., 2005). In neurons, LPA activates G-protein-coupled LPA receptors, elevates endogenous Rho within seconds, and induces growth cone collapse (Kozma et al., 1997; Kranenburg, 1999). In *Xenopus* neurons, LPA-induced growth cone collapse and repulsive steering in a gradient of LPA are abolished by TxB and when neurons express dominant-negative RhoA but not dominant-negative Cdc42 (Yuan et al., 2003), thus linking LPA and Rho-mediated turning in *Xenopus* growth cones. Since Rho inhibition attenuated cathodal growth cone turning (Fig. 2), we used LPA to determine if stimulating Rho activity enhanced cathodal turning. Unexpectedly, 1 μM LPA had no effect (data not shown). At a lower concentration (100 nM), LPA attenuated the angle and frequency of turning (Fig. 2A,B,D) but increased the migration rate (Fig. 2C).

Therefore, a high concentration of C3 transferase (20 μg/ml) attenuated turning, a high concentration of LPA (1 μM) allowed turning and lower concentrations of C3 transferase (1 μg/ml) and LPA (100 nM) attenuated turning. These data suggest that a critical balance of Rho activation and inactivation is essential for cathodal guidance. This idea is supported by the observation that the neurite paths of 100 nM LPA (Fig. 2D) and 1 μg/ml C3-transferase-treated neurons (n=91, data not shown) are wavy, suggesting that episodes of cathodal turning are interspersed with episodes of adaptation, as has been proposed for *Xenopus* growth cone chemotropism (Ming et al., 2002).

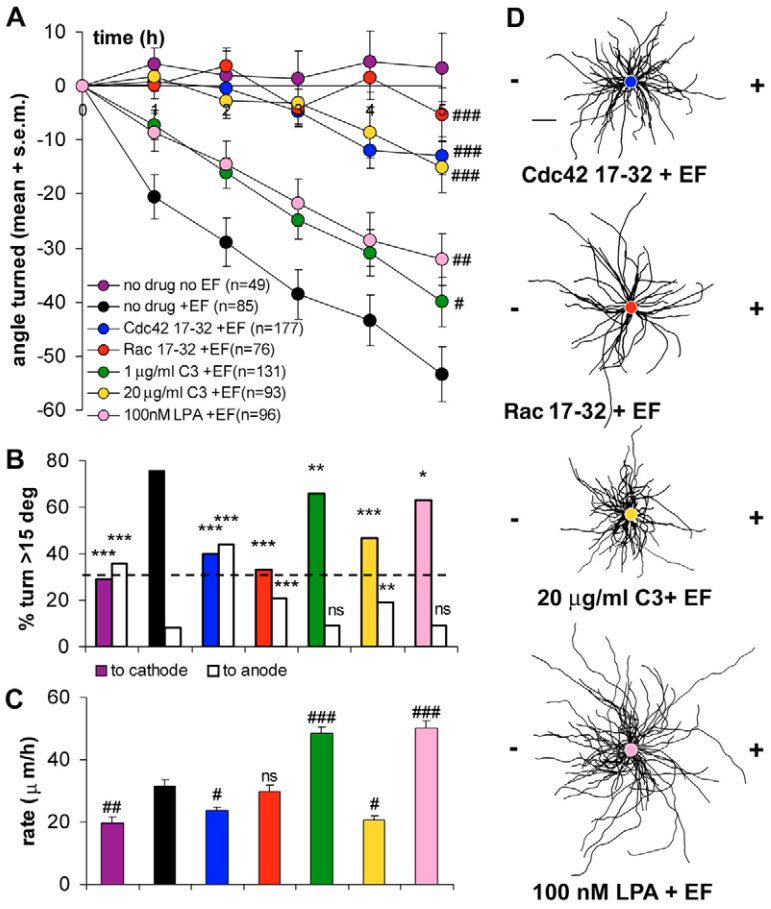

Fig. 2. Effect of selective inhibition of Rac, Rho or Cdc42 and elevation of Rho on EF growth cone guidance. See Fig. 1 for format. No drug + EF data are repeated from Fig. 1 for ease of comparison. (A) Mean angle turned since the start. $^{\#}P$<0.05; $^{\#\#}P$<0.005; $^{\#\#\#}P$<0.0001. (B) Frequency of cathodal (filled bars) and anodal (open bars) turning compared with no drug + EF (black bar). *P<0.05; **P=0.002; ***P<0.001. (C) The rate of neurite extension in an EF for 5 hours. $^{\#}P$<0.005; $^{\#\#}P$=0.0035; $^{\#\#\#}P$<0.0001. (D) Composite drawings of neurite paths for EF-treated cells. Compare with no drug in Fig. 1D. Bar, 100 μm for all drawings. ns, not significant.

RhoA immunofluorescence is higher anodally

If asymmetric Rho signalling mediates cathodal growth cone turning in a manner analogous to chemotropism (Jin et al., 2005) then Rho activity would be enhanced anodally. We tested this notion by measuring relative Rho immunofluorescence in anode-facing and cathode-facing sides of growth cones (single plane confocal images). Rho levels were expressed as the ratio of anode-to-cathode immunofluorescence. A symmetrically fluorescent growth cone would have an intensity ratio of 1 but, if Rho fluorescence were higher anodally, the ratio would be >1 and, if it is higher cathodally, the ratio would be <1. Rho fluorescence was uniform in control growth cones (no EF no drug; ratio=1.07±0.06, n=15) but was higher anodally than cathodally in EF-treated growth cones (1.51±0.11, n=10; P=0.0013). Similarly, Rho fluorescence in 100 nM LPA was uniform without an EF (0.98±0.04; n=5) but was elevated anodally in an EF (1.21±0.04, n=61; P=0.0017). When considered collectively (regardless of LPA), Rho

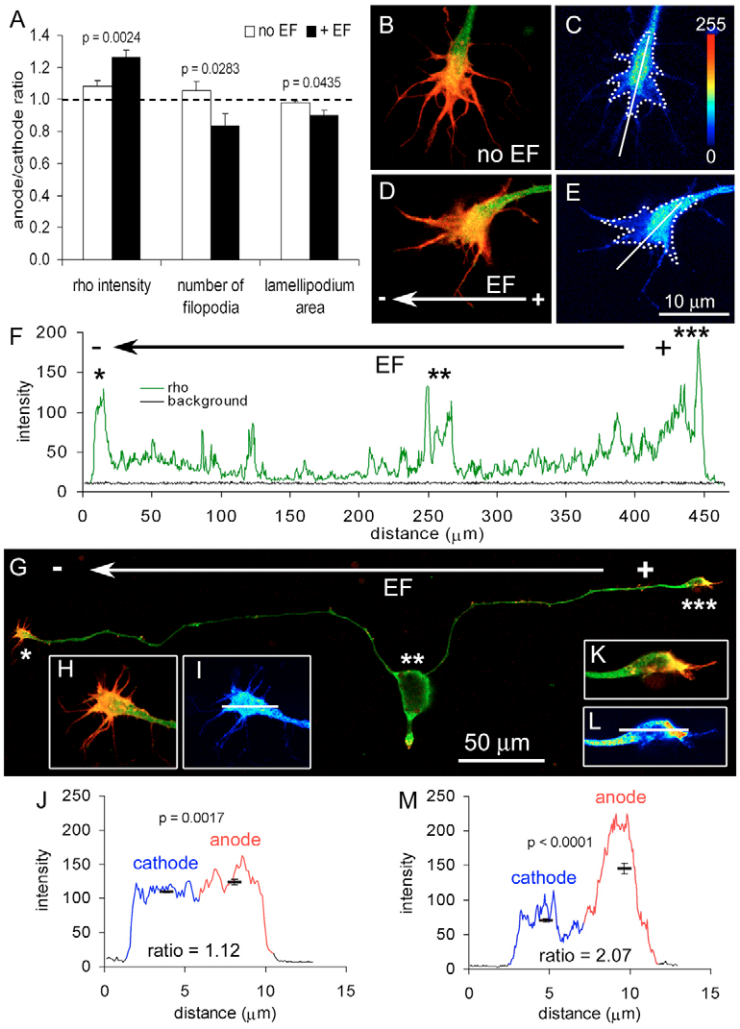

Fig. 3. Anodal RhoA elevation correlates spatially with collapsed morphology. (A) Mean anode-to-cathode ratios for Rho immunofluorescence intensity, number of filopodia and lamellipodial area for 40 growth cones (350 total filopodia) oriented within 45° of the EF direction and 13 growth cones with no EF (182 total filopodia). *P* values (p; two-tailed Student's *t* test) compare no EF and +EF ratios. A ratio of 1.0 (dotted line) indicates a symmetric growth cone, whereas ratios >1 and <1 indicate relative anodal and cathodal bias, respectively. (B,D) Confocal images of growth cones in100 nM LPA labelled with Rhodamine-phalloidin (red) and an antibody to RhoA (green). Image planes have been merged. (C,E) Confocal image of RhoA immunofluorescence with fluorescence intensity pseudocoloured on the scale shown. Dotted outlines indicate the regions used to calculate ratios. (F) RhoA immunofluorescence intensity plot for the cell in G. The green line represents Rho fluorescence measured along a line extending from the tip of the cathode-facing growth cone, along the neurite contour to the tip of the anode-facing growth cone. The black line represents fluorescence intensity when the same line is shifted to a background position near, but not overlapping, the cell. Asterisks indicate corresponding regions in image G. (G) A neuron in an EF for 5 hours labelled as in B. Insets (H,I,K,L) show detail of cathode-facing and anode-facing growth cones. (J,M) Fluorescence intensity plots for the lines indicated on I and L. Mean intensities (±s.e.m.) for the cathode-facing (blue) and anode-facing (red) sides of each plot are indicated by black bars. Ratios indicate mean anode intensity compared with mean cathode intensity for each growth cone. Cathode- versus anode-facing means were compared with a two-tailed Student's *t* test.

fluorescence was uniform in growth cones without an EF but was elevated anodally in EF-treated growth cones (Fig. 3A).

Collapse of the anode-facing sides of growth cones correlates temporally with cathodal turning (Rajnicek et al., 2006). We therefore examined the spatial relationship between EF-induced Rho immunofluorescence and growth cone morphology (Fig. 3). Only growth cones oriented at a right angle to the EF direction (90±45°, some with LPA) were included. We counted the filopodia and measured the lamellipodial area (excluding filopodia) of the cathode- and anode-facing regions from which Rho immunofluorescence had been determined. Each was expressed as a ratio of the anode-to-cathode values for individual growth cones (Fig. 3A). In 13 control (no EF) growth cones, the Rho immunofluorescence intensity, distribution of filopodia and lamellipodial area were symmetrical (ratio ~1.0) but, in 40 EF-treated growth cones, elevation of Rho on the anode-facing sides correlated spatially with anodal reduction of filopodia and lamellipodia.

Rho activation induces growth cone collapse and neurite retraction (Kozma et al., 1997; Thies and Davenport, 2002; Kranenburg et al., 1999); therefore, anodal accumulation of Rho would be predicted to cause anode-facing growth cones to collapse and either to retract or advance more slowly than cathode-facing ones. Our data and a previous report (McCaig, 1987) support these ideas. Growth cones rarely faced the anode after 5 hours of EF exposure, but Fig. 3 shows a neuron whose growth cones faced the cathode and anode directly. The Rho immunofluorescence gradient in the cathode-facing growth cone (* in Fig. 3F,G) was less steep (ratio 1.12) and it had a more complex morphology than the relatively collapsed anode-facing growth cone (*** in Fig. 3F,G), which had a steeper Rho fluorescence gradient (ratio 2.07). Rho immunofluorescence is higher in the shorter (180 μm), anode-facing neurite than the longer (245 μm), cathode-facing neurite (Fig. 3F), suggesting a link between Rho elevation and reduced anodal migration rate. Our time-lapse data support this notion. Of 85 EF-treated growth cones in the present study, only two faced the anode at 5 hours and these migrated at 3.1±0.2 μm/hour compared with 33.0±2.4 μm/hour for 71 growth cones facing cathodally. Therefore, compared with growth cones without an EF (19.6±2.1 μm/hour, *n*=49), cathodal rates increase and anode-facing growth cones migrate very slowly. If Rho activity underlies reduced rates, then C3 transferase inhibition of Rho should 'rescue' anode-facing growth cone advance. Indeed, in 1 μg/ml C3 transferase, anode-facing growth cones migrate faster (61.3±16.1 μm/hour, *n*=6) than cathode-facing growth cones (17.5±2.2 μm/hour, *n*=100, *P*=0.0440) and, in 20 μg/ml

Journal of Cell Science

C3 transferase, rates are identical in each direction (22.1±1.0 μm/hour, n=14 anodally and 18.3±1.5 μm/hour, n=42 cathodally). Therefore, Rho inhibition rescues anodal attenuation of growth cone advance.

Inhibition of RhoA effectors

Having established a role for RhoA in cathodal turning, we explored the effector molecules that Rho might use to direct cytoskeletal dynamics. We used 10 μM Y27632 (Uehata et al., 1997) to inhibit p160 ROCK, which mediates growth cone collapse in response to Rho activation (Wahl et al., 2000) and two cell-permeable peptides, Rho 23-40 and Rho 75-92, corresponding to the binding sites for citron-K and rhophilin-rhotekin-PKN, respectively (Fujisawa et al., 1998), thereby preventing their downstream signalling. Y27632 (10 μM) has been used previously to implicate ROCK in Rho-mediated *Xenopus* growth cone chemotropism (Yuan et al., 2003). Y27632 (10 μM) and Rho 23-40 (10 μg/ml) each abolished cathodal turning during the first 2 hours, but not between 2 and 5 hours (Fig. 4A,B,D), which is consistent with our observation that Rho signalling is especially important in the initial 2 hours of EF exposure (Fig. 2A). With Y27632 and Rho 23-40, the extent of growth cone turning in 2 hours was the same as that without an EF (–4±3° and –2±2°, respectively). 26% (38/145) of growth cones turned cathodally in Y27632 and 30% (86/289) turned cathodally in Rho 23-40 (Fig. 4A). Turning resumed at 2 hours and, by 5 hours, the angle and frequency of cathodal turning were similar in each inhibitor (Fig. 4A,B). Neurite growth rates were unchanged in 10 μM Y27632 but increased in Rho 23-40 compared with EF-treated growth cones without inhibitor (Fig. 4C). 5 μM Y27632 had no effect on growth cone turning (–48±4° at 5 hours) but it increased the migration rate to 53.0±2.0 μm/hour (P<0.0001, n=231).

The Rho 75-92 peptide decreased, but did not abolish, the early phase of cathodal turning (Fig. 4A). For example, growth cones turned only –12±3° in Rho 75-92 by 2 hours compared with –29±4° without the peptide (P=0.0008). By 5 hours, the angle and frequency of cathodal turning were not different to EF-treated cells without the peptide (Fig. 4A,B). Collectively, these data implicate Rho activity (especially the citron-K-binding domain) in cathodal turning and suggest that the early phase requires p160 ROCK activity linked to Rho activation.

The ability of Rho 23-40 to abolish the early phase of turning yet Rho 75-92 permitted limited cathodal turning, together with the distinct inhibitory responses of Rac 17-32 and Cdc 17-32 described above, further suggest that the presence of the TAT sequence is not responsible for the effects of the peptides.

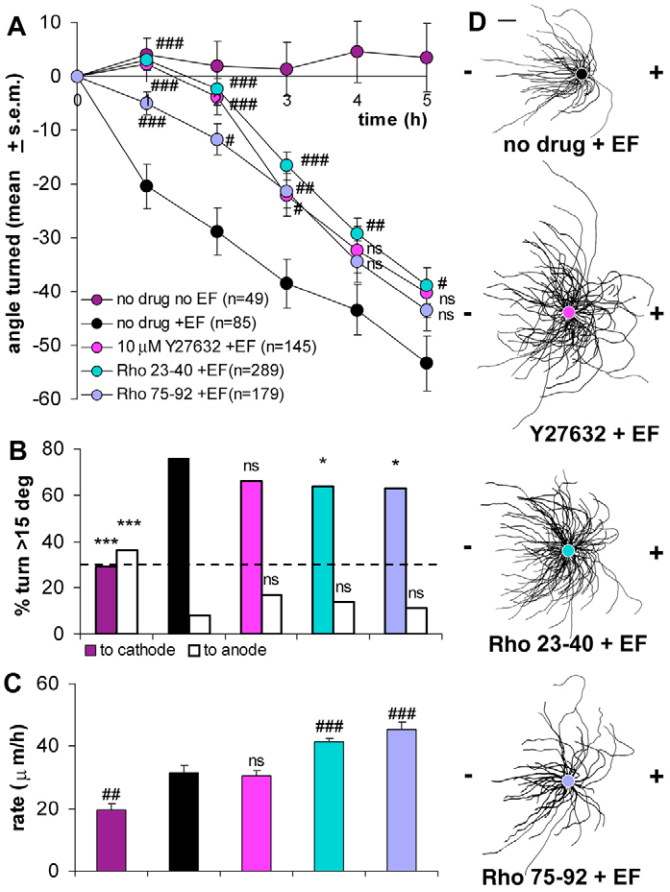

Fig. 4. Inhibition of Rho effectors attenuates EF-induced growth cone guidance. Format is as in Fig. 1. (A) Mean angle turned during 5 hours. No drug + EF data are repeated from Fig. 1 for comparison; ns, not significant; $^{\#}P$<0.05; $^{\#\#}P$=0.0002; $^{\#\#\#}P$<0.0001. (B) Frequency of cathodal or anodal turning. *P<0.05; ***P<0.001. (C) Rate of growth cone advance in an EF. $^{\#\#}P$=0.0002; $^{\#\#\#}P$<0.0001. (D) Composite drawings of neurons in an EF (cathode to the left) for 5 hours. Compare with no drug + EF in Fig. 1D. Bar, 100 μm for all drawings.

MLCK is involved in early turning

Having revealed roles for Rac, Cdc42 and Rho signalling in cathodal orientation (Figs 1, 2) we explored the potential involvement of effector molecules downstream from these GTPases. Wortmannin (500 nM) (Davies et al., 2000) and butanedione monoxime (BDM) (2 mM), an inhibitor of myosin ATPase (Herrmann et al., 1992), were used to inhibit myosin light chain kinase (MLCK) activity. BDM has been used previously in studies of *Xenopus* growth cones to implicate MLCK in motility (Ruchhoeft and Harris, 1997) and to reveal that Cdc42 and Rho signals converge at MLCK to underpin steering in chemical gradients (Yuan et al., 2003). DMSO was used as a solvent for wortmannin and other inhibitors used in this and the companion paper in this issue (Rajnicek et al., 2006), so the influence of DMSO on cathodal growth cone migration was tested from 0.0004% to 0.3% DMSO to reflect the range of solvent concentrations in the medium. The cathodal responses did not vary within this range so data were pooled. Over the 5 hours of EF exposure in DMSO-containing medium, the angle turned (Fig. 5A, Fig. 6A) and the frequency of cathodal turning were the same as without DMSO (Fig. 5A,B, Fig. 6A,B), but growth cones migrated faster in DMSO than without it (Fig. 5C, Fig. 6C).

Wortmannin (0.1% DMSO final concentration) or BDM (dissolved directly in culture medium) attenuated, but did not abolish, cathodal turning during the first 3 hours (Fig. 5A). Attenuation was quantitatively and temporally similar for both drugs. At 2 hours, growth cones in 500 nM wortmannin turned only –11±4° with 35% (39/111) to the cathode, significantly less (P=0.0034 and P<0.002, respectively) than in DMSO (–23±2°, 57% 249/440). Similarly, in BDM, they turned only –8±2° with 30% (44/147) compared with –29±4° and 72% (61/85) without the drug. However, by 5 hours, the mean angle

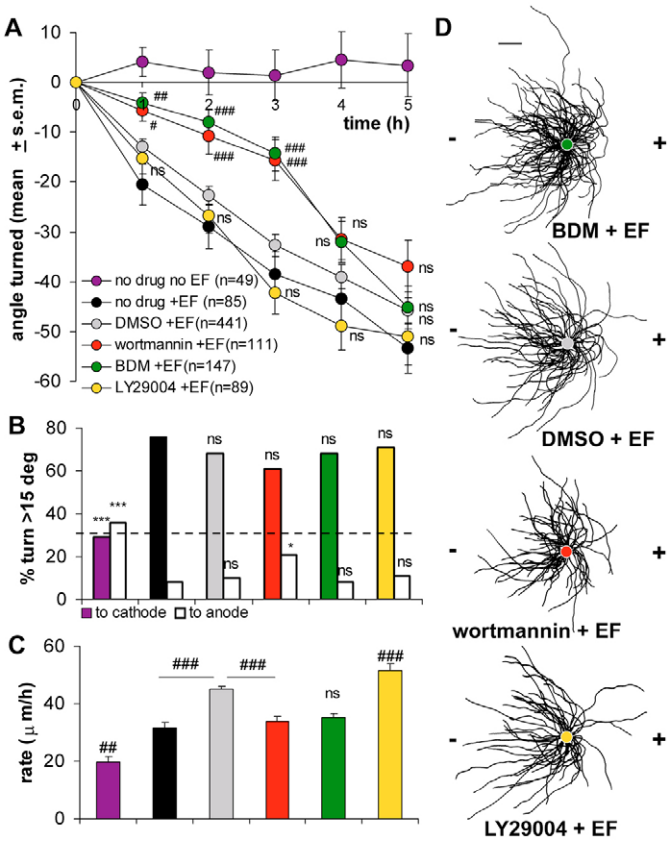

Fig. 5. Effects of inhibition of myosin-based contraction (using BDM or wortmannin) or PI 3-kinase (using LY294002 or wortmannin) on EF-induced growth cone guidance. Formatted as in Fig. 1. No drug + EF data are repeated from Fig. 1; ns, not significant compared with revelant no drug + EF or DMSO + EF control. (A) Mean angle turned. $^{\#}P<0.05$; $^{\#\#}P<0.0004$; $^{\#\#\#}P<0.0001$. (B) Frequency of turning during 5 hours. $^{*}P<0.05$; $^{***}P<0.001$. (C) Growth rates during 5 hours of EF exposure. $^{\#\#}P=0.0002$ compared with no drug + EF (black bar); $P<0.0001$ compared with DMSO + EF (grey bar). (D) Composite drawings of neurons in an EF (cathode to the left) for 5 hours. Bar, 100 μm for all drawings. Compare BDM and DMSO drawings to no drug + EF in Fig. 1D, and compare wortmannin and LY294002 to DMSO.

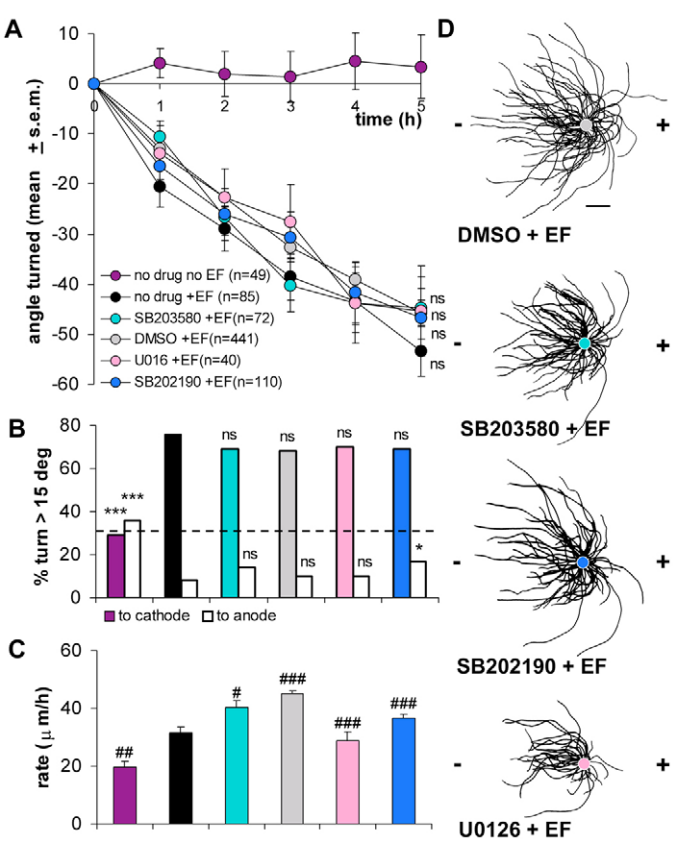

Fig. 6. Effect of inhibition of MAPK signalling on EF-induced growth cone guidance. Format as is Fig. 1. Control data are repeated from Fig. 1; ns, not significant. (A) Mean angle turned during 5 hours is not affected by any inhibitor. (B) Percentage of growth cones that turn cathodally or anodally during 5 hours. None of the inhibitors affected the frequency of cathodal turning and only SB202190 slightly increased the anodal frequency compared with the DMSO control; *, $P<0.05$; $^{***}P<0.0001$. (C) Rate of growth cone advance during 5 hours in an EF. P values compared with no drug + EF: DMSO, $^{\#\#\#}P<0.0001$; SB203580, $^{\#}P<0.05$. P values compared with DMSO + EF: U0126 and SB202190, $^{\#\#\#}P<0.001$. (D) Composite drawings of neurons in an EF (cathode to the left) for 5 hours. Bar, 100 μm for all drawings. Compare U0126 and SB202091 to DMSO at top of panel and compare SB203580 to no drug + EF in Fig. 1D.

and the frequency of turning were not different compared with the relevant controls (Fig. 5A,B,D). A lower concentration of wortmannin (5 nM, n=87) yielded similar results. The frequency of cathodal turning was reduced at 2 hours (44%, 38/87) compared with DMSO controls ($P<0.05$) but not at 5 hours (61%, 53/87 in 5 nM wortmannin; 68% 301/440 in DMSO). The angle turned in 5 nM wortmannin was not significantly different to the angle turned in 500 nM wortmannin. By 5 hours, growth cones had turned –30±6° in 5 nM wortmannin compared with –37±5° in 500 nM. The rate of growth cone migration in BDM was identical to controls with no drug but it was decreased by 500 nM (Fig. 5) or 5 nM wortmannin (27.5±1.3 μm/hour) compared with DMSO (45.0±1.1 μm/hour; P=0.0013). These data implicate MLCK activity in cathodal turning during the early phase.

PI 3-kinase activity is not essential for cathodal turning

PI 3-kinase is activated by Rac during chemotaxis (Servant et al., 2004), and the specific PI 3-kinase inhibitor LY294002 attenuates cathodal migration of epithelial cells (Zhao et al., 2002) and mediates adaptation of *Xenopus* growth cone turning in chemical gradients (Ming et al., 2002). We therefore used LY294002 (10 μM) to inhibit PI 3-kinase (Vlahos et al., 1994; Davies et al., 2000) in EF-treated neurons. Although LY294002 enhanced the rate of growth cone migration in an EF (Fig. 5C), it did not affect the angle (Fig. 5A,D) or the frequency (Fig. 5B) of cathodal turning. These responses are different than those in wortmannin, a less specific inhibitor of PI 3-kinase (Davies et al., 2000), which reduced cathodal turning during the early phase and slowed growth cone advance (Fig. 5). Therefore, we conclude that PI 3-kinase signalling is not required for either phase of cathodal growth cone steering and the effect of wortmannin on cathodal orientation is not a result of inhibition of PI 3-kinase.

Journal of Cell Science

MEK1/2 and p38 MAPK signalling are not required for cathodal turning

MEK1/2, ERK1/2 and p38 MAPK (p38) signalling have been implicated in cathodal migration of epithelial cells (Wang et al., 2003; Zhao et al., 2002) and chemoattraction of *Xenopus* growth cones (Campbell and Holt, 2003; Ming et al., 2002), so we tested their involvement in EF growth cone guidance with the same inhibitors used for studies of *Xenopus* growth cone chemoattraction (Campbell and Holt, 2003; Ming et al., 2002). ERK1/2 activation by MEK1/2 was inhibited using 30 μM U0126 (0.3% DMSO) (Duncia et al., 1998), whereas p38 was inhibited using 300 nM SB202190 (0.003% DMSO) or 10 μM SB203580 (dissolved in culture medium) (Davies et al., 2000). None of these inhibitors affected the mean angle turned or the frequency of cathodal turning (Fig. 6A,B,D). Growth cones migrated faster in SB203580 and SB202190 than without any drug but they were slower in U0126 than in DMSO alone (Fig. 6C). Antibody staining (not shown) confirmed ERK1 and p38 MAPK presence in growth cones. Immunofluorescence of total p38 MAPK (active and inactive, assessed as for total Rho) was uniform (ratio=0.96±0.07, n=6) across EF-treated growth cones oriented at a right angle to the EF (90±45°), suggesting that the EF does not induce a gradient of total p38 MAPK. Together with the pharmacological data, this indicates that p38 MAPK and ERK1/2 signalling are not essential for directed cathodal growth cone migration.

Discussion

We demonstrate that the GTPases Cdc42, Rac and Rho mediate growth cone steering in a physiological EF by spatiotemporal regulation of GTPase activity and their effectors. In the companion paper in this issue (Rajnicek et al., 2006), we describe the cytoskeletal requirements for EF steering, the effects of inhibition of Rac and Cdc42 signalling on asymmetric growth cone morphology and the consequences for EF guidance. The present study expands understanding of the cathodal guidance mechanism considerably by establishing a requirement for seven additional pathway components (Cdc42, Rac, Rho, p160 ROCK, citron-K, rhophilin-rhotekin-PKN and MLCK), eliminating three others (p38 MAPK, ERK1/2 and PI 3-kinase) (Fig. 7A,B) and demonstrating an EF-induced asymmetry of total RhoA, but not p38 MAPK, in EF-treated growth cones. It also highlights similarities and differences in the signal transduction mechanisms for growth cone guidance by chemical and electrical gradients, suggesting that these directional cues, which co-exist during development and regeneration, might be integrated or interpreted selectively.

Proposed mechanism for growth cone guidance by an EF

During development and regeneration, growth cones integrate multiple, co-existing, extracellular cues to find appropriate synaptic targets (reviewed by Yamamoto et al., 2003; Patel and Van Vactor, 2002; Mueller, 1999). The most frequently studied guidance cues are diffusible or substratum-bound chemical gradients, but the naturally occurring EF of 400-1000 mV/mm in the developing (Hotary and Robinson, 1991; Hotary and Robinson, 1992; Shi and Borgens, 1994) and regenerating (Song et al., 2004) nervous system is often neglected. This stems, in part, from misunderstanding or ignorance of the basic physiological principles of bioelectricity (reviewed by McCaig et al., 2005). DC EFs merit serious consideration because an endogenous EF is present for sustained periods during normal development and its disruption perturbs normal nervous system development (Hotary and Robinson, 1992; Hotary and Robinson, 1994); furthermore, EFs co-exist with the other types of guidance cues mentioned above. Although the ability of an EF to enhance neuronal differentiation, determine the direction of amphibian (*Xenopus*) growth cone migration and neurite branching is long established (e.g. Hinkle et al., 1981; Patel and Poo, 1982; Rajnicek et al., 1998), the mechanism by which growth cones detect and translate small voltage gradients into cathodal migration remains largely unknown.

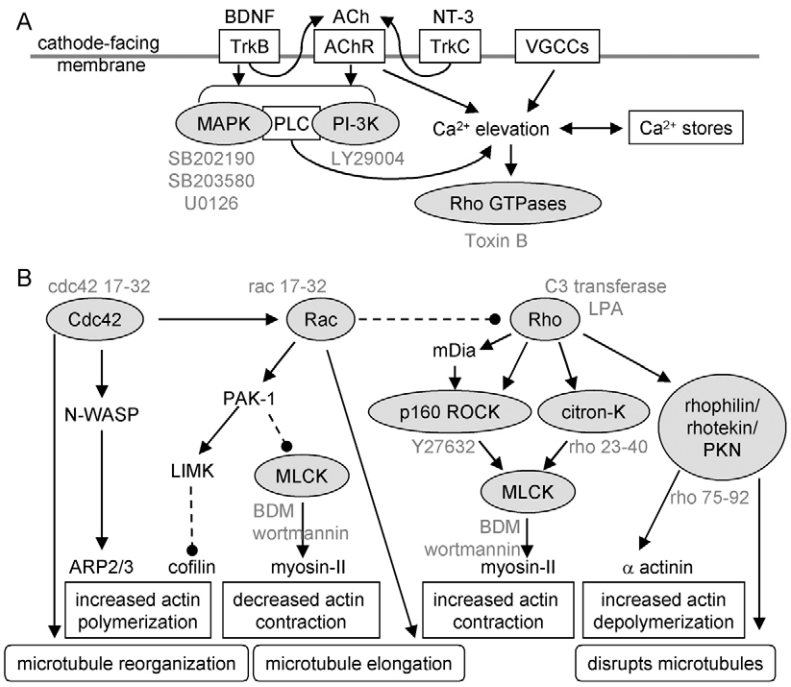

Fig. 7. Working model for cathodal growth cone turning in an EF. See Discussion for detail. (A) The current model for growth cone steering of *Xenopus* growth cones by an EF. Pathway components implicated previously in cathodal turning are in boxes and grey ovals indicate components explored in the present study. Pharmacological inhibitors used in the present study are shown in grey text at their points of action. (B) Proposed pathway linking Rho GTPase activity to cathodal turning. In this scheme, Cdc42 and Rac signalling dominate cathodally, with concurrent suppression of Rho. Conversely, Rho signalling dominates anodally, with suppression of Cdc42/Rac activity through Rho activation (not shown). Thus, on the anode-facing side of the growth cone, the signalling events and consequences on cytoskeletal dynamics would be opposite to those indicated. Pathway components studied in this study are indicated in grey ovals and the inhibitors used (with the exception of LPA, which activates Rho) are indicated in grey text at their sites of action. Although the pathways are roughly linear for ease of presentation, extensive cross-talk would be expected.

Journal of Cell Science

Hypothetical model for cathodal steering

The current model for EF-induced growth cone steering is presented in Fig. 7A. Central to the scheme is the premise that asymmetric activity of membrane proteins arises either by selective cathodal activation or by accumulation of specific proteins in the cathode-facing membrane. This idea is based on the finding that ACh receptors (AChRs) move rapidly to the cathode-facing side of cells (Orida and Poo, 1978) and AChR activity is required for EF growth cone guidance (see below). Candidate proteins include those whose activities are essential for cathodal guidance of *Xenopus* growth cones. In addition to the AChR, they include TrkB (the BDNF receptor), TrkC (the NT-3 receptor) and voltage-gated Ca^{2+} channels (VGCCs). AChR activity and Ca^{2+} elevation are linked in this scheme. Growth cones release ACh spontaneously, which binds to the AChR, activating a signalling cascade that includes MAPK, PLC and PI 3-kinase, elevating cytoplasmic Ca^{2+}, which is elevated further by the AChR itself, which is 'leaky' to Ca^{2+}. Activation of TrkB and TrkC induce release of ACh from the growth cone, which activates the AChR, further elevating Ca^{2+}. Elevated Ca^{2+} induces an additional Ca^{2+} rise through Ca^{2+}-induced Ca^{2+} release from thapsigargin and ryanodine-sensitive intracellular stores. The absolute requirement for Ca^{2+} in EF-induced guidance of growth cones has been disputed by Palmer et al. (Palmer et al., 2000) but they assessed overall neurite orientation after 12 hours rather than dynamic growth cone turning. We revealed differences in the signals that underpin cathodal steering in the initial 2 hours and >2 hours. The time-lapse studies used to develop the prevailing model of growth cone chemotropism (Song and Poo, 2001) are short; typically 30 to 60 minutes (e.g. Wen et al., 2004; Ming et al., 2002; Campbell and Holt, 2003), so it would be interesting to determine whether chemotropic signalling requirements change temporally in a manner similar to EF growth cone steering.

There are several unknown elements in the EF guidance scheme (Fig. 7A). For example, PLC activity is essential for cathodal turning (Erskine et al., 1995), but it is not known whether cathodal steering through TrkB and AChR activation involves MAPK and PI 3-kinase activity. How these collective signals regulate cytoskeletal dynamics to steer growth cones cathodally is unknown. We explored these questions by inhibiting components of the signalling pathway presented in Fig. 7B coupled with studies (Rajnicek et al., 2006) of inhibition of cytoskeletal dynamics and the roles of Rac and Cdc42 on regional growth cone morphology and cathodal steering.

p38 MAPK, ERK1/2 and PI 3-kinase activities are not required for cathodal steering

We tested the roles of p38 MAPK, ERK1/2 and PI 3-kinase in cathodal growth cone steering (Fig. 7A) for several reasons: (1) MAPK and PI 3-kinase are activated upon activation of TrkB and AChRs (Li et al., 2005), which mediate *Xenopus* growth cone steering in chemical and electrical gradients; (2) Rac activation stimulates PI 3-kinase during neutrophil chemotaxis (Servant et al., 2004); (3) PI 3-kinase and p38 MAPK activities are required for *Xenopus* growth cone turning in chemical gradients (Campbell and Holt, 2003; Ming et al., 2002); and (4) cathodal migration of epithelial cells requires ERK1/2 and PI 3-kinase (Wang et al., 2003; Zhao et al., 2002).

Surprisingly, we failed to identify roles for these molecules in cathodal growth cone turning (Figs 5, 6). This indicates that the molecular mechanisms underpinning cathodal migration differ in epithelial cells and growth cones. Although the intracellular mechanisms that mediate *Xenopus* growth cone steering in chemical and electrical gradients share components such as TrkB, TrkC, AChR and Rho GTPases, they differ in others, including nerve growth factor receptors, PI 3-kinase, p38 MAPK and ERK1/2 (McCaig et al., 2005). This suggests the possibility that, in embryos, where chemical and electrical gradients co-exist, growth cones might interpret the gradients separately, or perhaps combine them through molecular crosstalk, yielding net behaviours that enhance, integrate or negate individual guidance responses.

The Rho GTPases Cdc42, Rac and Rho are involved in growth cone steering

Our observation that collective inhibition of Rac, Rho and Cdc42 with TxB attenuates turning (Fig. 1) implicates them all in the EF response. Rho GTPase activation might be regulated by spatial changes in cytoplasmic Ca^{2+} (Henley and Poo, 2004; Jin et al., 2005) and provide a mechanism by which localised increases can be coupled to regional cytoskeletal dynamics (Patel and Van Vactor, 2002). Furthermore, the GTPases are activated in a cascade whereby GTP-Cdc42 activates Rac and GTP-Rac inactivates Rho (Raftopoulou and Hall, 2004). Rho activation is accompanied by de-activation of Cdc42, which amplifies the intracellular signalling gradient induced by the extracellular electrical gradient, yielding changes in cytoskeletal dynamics and membrane insertion that underpin growth cone steering (Giniger, 2002). Consistent with studies in which pharmacological manipulation of Rho activity with LPA mediated chemotropism of *Xenopus* growth cones (Yuan et al., 2003), and our observation that total RhoA is elevated anodally (Fig. 3), we hypothesise that the electrical gradient activates the Cdc42 and/or Rac pathway cathodally (with consequent inactivation of Rho) and Rho is activated on the anode-facing side of the growth cone (with consequent inactivation of Cdc42/Rac). This hypothesis is appealing because, unlike chemical gradients, electrical gradients simultaneously provide an attractive cue cathodally and a repulsive cue anodally to amplify the signalling gradient within the growth cone. Several lines of evidence support the notion that a Cdc42/Rac versus Rho gradient underpins cathodal steering: (1) a gradient of (but not global) AChR activation induces growth cone filopodia and lamellipodia in a Cdc42/Rac-dependent manner (Kozma et al., 1997); (2) Ca^{2+}-dependent ACh release is mediated by Rac, not Rho (Doussau et al., 2000); (3) ACh release and AChR activation are required for cathodal turning (Erskine and McCaig, 1995; McCaig et al., 2000); and (4) Rac-dependent filopodial asymmetry (increased cathodally) (Rajnicek et al., 2006) mediates cathodal growth cone steering.

How does asymmetric GTPase activity bias growth cone advance cathodally?

The mechanism for selective activation of Cdc42 and Rac cathodally is not clear but in the context of proven roles for activation of TrkB (the BDNF receptor), TrkC, AChR, VGCCs and Ca^{2+} release from stores (Stewart et al., 1995; McCaig et al., 2000), it is likely that local Ca^{2+} elevation triggers cAMP-

Journal of Cell Science

dependent protein kinase A (PKA) activation. PKA mediates chemoattraction of *Xenopus* growth cones in a BDNF gradient (Song et al., 1997) and PKA activates (indirectly) Cdc42 and Rac but inactivates Rho (Howe, 2004); thus, enhancing PKA activity cathodally could regulate attractive cathodal turning. Palmer et al. found that PKA inhibition or stimulation promoted cathodal neurite orientation after 12 hours but they did not measure dynamic growth cone turning so the role of PKA remains equivocal (Palmer et al., 2000). Furthermore, overexpression of inactive Cdc42 but not Rho prevents steering of *Xenopus* growth cones by a gradient of intracellular Ca^{2+} (Jin et al., 2005), providing a causal link between spatial regulation of Ca^{2+}, Rho GTPase activity and growth cone steering. However, the role of PKA in Ca^{2+} regulation of Rho GTPases was not examined.

A simplified scheme that might underlie cathodal growth cone turning is presented in Fig. 7B. On the cathode-facing sides of growth cones, Cdc42 is activated as a consequence of Ca^{2+} elevation (and possibly PKA), which activates the N-WASP–ARP2/3 pathway, causing actin nucleation and filopodial and lamellipodial extension. Our data (Fig. 2) implicate the CRIB domain of Cdc42 in this pathway. Cdc42 activation stimulates Rac activation (also perhaps through PKA) and GTP-Rac stimulates PAK-1. PAK-1 activates LIM kinase (LIMK), which inactivates the actin-severing protein cofilin, thereby increasing net actin polymerisation. In parallel, PAK-1 inhibits MLCK, which prevents myosin-II-based contraction of the actin network. Here, we provide evidence for roles for the CRIB domain of Rac (Fig. 2A) and MLCK (Fig. 5A). Rac activation inhibits Rho activation (Raftopoulou and Hall, 2002) in parallel with PKA inhibition of Rho, which prevents collapse of the cathode-facing growth cone and favours extension towards the cathode.

RhoA involvement in cathodal growth cone guidance

How does the EF influence events on the anodal sides of growth cones? We propose that RhoA is redistributed (Fig. 3) and/or activated locally by an unidentified mechanism. This might result from relatively low cytoplasmic Ca^{2+} affecting nucleotide exchange (Henley and Poo, 2004). The result is net activation of Rho and stimulation of p160 ROCK and MLCK, with a tendency to growth cone collapse (Fig. 7B). Support for this idea is provided by the present study because: (1) total Rho immunofluorescence was higher on the anode-facing sides of growth cones (Fig. 3F); (2) elevated Rho correlated spatially with a collapsed growth cone morphology (Fig. 3E,G); (3) Rho inhibition with C3 transferase (Fig. 2) attenuated cathodal turning and 'rescued' anodal attenuation of migration rates; and (4) inhibition of p160 ROCK (Fig. 4) or MLCK (Fig. 5) abolished or attenuated early turning.

Neurites in low concentrations of the Rho inhibitor (C3 transferase) or the Rho activator (LPA) migrated in 'zig-zag' patterns in an EF (Fig. 2D) and LPA attenuated cathodal turning (Fig. 2A), suggesting that tight regulation of Rho or its effectors is essential for cathodal guidance. Although our immunofluorescence data (Fig. 3D) are not specific for active Rho, the increased concentration of total Rho anodally suggests that, even if the EF elevated Rho uniformly, it is probable that Rho-GTP would be higher anodally.

We addressed this issue using western blots from neural tubes (20 in each case) that were either exposed to an EF or not (data not shown). The EF elevated total Rho compared with no EF controls but less than when exposed to LPA (no EF), which activates Rho globally. This is consistent with, but does not prove (see below), the idea that Rho is elevated anodally by an EF. We did not measure Rho activation in neurons biochemically because available assays use the rhotekin-binding site and in our study the peptide specific for the rhotekin site (Rho 75-92) was the least effective at blocking cathodal guidance (Fig. 4A). Moreover, whole-cell biochemical techniques would be insufficient to correlate Rho levels spatially with EF polarity.

Our pharmacological data (Figs 4 and 5) suggest a model (Fig. 7B) in which Rho activation of p160 ROCK, citron-K, MLCK and rhotekin-rhophilin-PKN are essential for EF steering, especially during the early phase. The quantitatively identical responses in Y27632 and Rho 23-40, and their similarity to the quantitatively identical responses in BDM and wortmannin, are consistent with the idea that these pathways converge mechanistically at MLCK. Rho-GTP activates p160 ROCK, leading to myosin-II-based contraction through MLCK, retrograde actin flow and collapse of the anode-facing side of the growth cone. In parallel, Rho induces activation of citron-K, which activates MLCK, further contributing to growth cone collapse. Rho activation of rhophilin-rhotekin-PKN signalling increases actin depolymerisation through α-actinin (Raftopoulou and Hall, 2004). In addition, PKN phosphorylates Tau, which destabilises microtubules (Taniguchi et al., 2001). Although citron-K regulates mouse cortical dendrite outgrowth (Di Cunto et al., 2003), we are not aware of any previous evidence for roles for PKN or citron-K in growth cone guidance.

Microtubules and GTPases

Although most emphasis has been on the effect of Rho GTPase activity on the actin cytoskeleton in growth cone guidance, microtubules are also important in path-finding (Lee et al., 2004; Gordon-Weeks, 2003; Raftopoulou and Hall, 2004). In the companion paper in this issue, we show that disruption of either microfilament or microtubule dynamics inhibits cathodal turning (Rajnicek et al., 2006), so we have incorporated microtubules into our hypothetical model (Fig. 7B). In addition to effects on microfilaments, Rho GTPases influence microtubule function and stability. For example, Rac and Cdc42 localise to the growing ends of microtubules, establishing polarisation of the leading edge during migration (Fukata et al., 2002), and promote microtubule elongation and dynamics cathodally.

In summary, we have revealed temporally and spatially distinct requirements for members of the Rho family of small GTPases (Rac, Rho and Cdc42) in growth cone guidance by EFs. Our data further suggest involvement of the effectors p160 ROCK and MLCK but not ERK1/2, PI 3-kinase or p38 MAPK. Rho is activated following brain injury in humans (Brabeck et al., 2004) or spinal cord injury in rats (Sung et al., 2003; Madura et al., 2004) and Rho inhibition in adult rats improved recovery from spinal cord injury (Brabeck et al., 2004; Fournier et al., 2003; Sung et al., 2003). These observations, in conjunction with the success of a recent clinical trial using EF stimulation to treat neurologically complete human spinal cord injuries (Shapiro et al., 2005), highlight the need to understand the potential interaction of these cues in growth cone guidance.

Journal of Cell Science

Materials and Methods

Cell culture

Generation of embryos and primary cultures of *Xenopus laevis* spinal neurons were described previously (Rajnicek et al., 1998). Embryos obtained by in vitro fertilisation were maintained in 5% DeBoer's solution (5.5 mM NaCl, 0.07 mM KCl, 0.02 mM $CaCl_2$, pH 7.2) at 12-23°C until stage 20-22 (Nieuwkoop and Faber, 1956). The jelly coat and vitelline envelope were removed and the dorsal third of the embryo (which contains the neural tube) was transferred to a solution of 1 mg/ml type I collagenase (Sigma) in Steinberg's solution [58 mM NaCl, 0.67 mM KCl, 0.44 mM $Ca(NO_3)_2$, 1.3 mM $MgSO_4$, 4.6 mM Trizma Base, pH 7.9]. Isolated neural tubes were disaggregated in Ca^{2+}-Mg^{2+}-free (CMF) Steinberg's (58 mM NaCl, 0.67 mM KCl, 4.6 mM Trizma Base, 0.4 mM EDTA, pH 7.9) then CMF was replaced with culture medium composed of 20% (v/v) modified Leibovitz L-15 medium without L-glutamine (ICN Biomedical), 2% (v/v) penicillin (5000 IU/ml)/streptomycin (5000 μg/ml), 1% (v/v) calf serum, 77% (v/v) Steinberg's solution (pH 7.9). Neural tubes were then triturated to yield a suspension of isolated neurons. Cells were plated directly into the central trough of the chamber described below and used for experiments when neurites were at least one cell diameter (~30 μm) long. In most cases, drug-containing medium was perfused through the chamber immediately before the first (0 hour) images were collected but in some cases (see below) drugs were perfused earlier.

Electric field application

A DC EF was applied to neurons using a chamber design that included agar-salt bridges to eliminate contamination of the culture medium by electrode products and to isolate cells from pH changes at the electrodes (McCaig et al., 2005). Experiments using a modification of this chamber proved that directional responses of growth cones are not caused by chemotropic gradients established within the culture chamber by the EF (Hinkle et al., 1981) since neurites still responded cathodally under perfusion, which prevented establishment of chemical gradients.

The chamber was a 100 mm tissue culture dish (Falcon) to which two strips of no 1 coverslip (64 mm long × 12 mm wide) were secured parallel to each other, 1 cm apart, with silicone adhesive (Dow Corning RTV 3140). The adhesive was allowed to cure at least 24 hours before plating cells into the central trough defined by the coverslips. A third coverslip (64 mm × 24 mm) was secured over the top of the cells using a non-curing silicone compound (Dow Corning DC4). This creates a rectangular EF chamber 64 mm long, 10 mm wide and ~0.5 mm high. Electrical contact to the cells was made through 15 cm long agar-salt bridges (glass tubing filled with 1% w/v agar in Steinberg's solution). One end of each bridge rested in a pool of culture medium continuous with that in the central trough of the chamber and the other end of each bridge rested in a beaker of Steinberg's solution containing a Ag/AgCl electrode connected to a DC power supply in series with a variable resistor. The EF used for all experiments was 150 mV/mm. The field strength was determined by measuring the voltage drop across the chamber at the start of the experiment. Drops of fresh medium (with or without pharmacological inhibitors) were added to the chambers coincident with hourly measurement of the EF strength. This prevented evaporation and replenished inhibitor-containing medium throughout the 5-hour experiment.

Pharmacological reagents

The following reagents were dissolved directly into culture medium: butanedione monoxime (BDM) (Sigma), C3 transferase from *Clostridium botulinum* (Biomol Research Labs), L-α-lysophosphatidic acid (LPA) (Sigma), SB230850.HCl (Tocris), toxin B (TxB) from *Clostridium difficile* (Sigma), Y27632 (Tocris). DMSO was the solvent for LY294002 (Sigma), SB202190 (Tocris), U0126 (Promega) and wortmannin (Sigma). Since wortmannin is light sensitive, the dish was covered with foil between hourly image acquisitions.

Four short peptide sequences corresponding to effector binding domains on RhoA, Rac 1 and Cdc42 were custom synthesised (University of Aberdeen Proteomics Facility, Aberdeen, UK). The synthesis, specificity and efficacy of these peptides in inhibiting their respective GTPase effector domains have been reported previously (Fujisawa et al., 1998; Vastrik et al., 1999). The peptides correspond to amino acids 23-40 of RhoA (the class III binding domain), amino acids 75-92 of RhoA (the class I binding domain), amino acids 17-32 of Rac 1, and amino acids 17-32 of Cdc42 (Rac and Cdc42 CRIB domains). Each peptide was tagged with the TAT internalisation sequence (GRKKRRQRRRPPQC) at its C-terminus to facilitate transport into the cytoplasm (Dunican and Doherty, 2001). The peptides were dissolved directly into culture medium. Neurons were pre-incubated in the peptides or C3 transferase for at least 1 hour prior to the experiment to allow uptake by the cells. The compounds had no effect on growth cone behaviour in EFs when incubated for shorter durations, suggesting that the cytoplasmic concentration of drug was too low to exert an effect at pre-incubation times less than 1 hour.

Analysis of growth cone turning

The angle of growth cone orientation relative to the horizontal EF was determined at hourly intervals for 5 hours. Digital images were captured using a Nikon Diaphot inverted phase contrast microscope equipped with a monochrome CCD TV camera coupled to Leica Quantimet imaging software. Images of identified cells were captured hourly, and measurements of neurite length and angle were made from printed images. The camera was aligned relative to the EF chamber so that the EF vector was horizontal, with the cathode to the left of each image and the anode to the right. Since growth cones tend to 'wobble' by about 10° during randomly directed growth (no directional cue), a growth cone was considered to have 'turned' if there was a net change in angle >15° since the start of the experiment. The mean angles turned were compared using a Student's two-tailed *t* test. The frequency of growth cones turning toward the cathode, anode, or failing to turn were compared using a D-test (Bailey, 1981). The expected frequency in each of the three categories would be 33% for a population of growth cones migrating randomly.

Confocal microscopy

Cells were fixed and permeabilised simultaneously for 20-30 minutes in 4% (v/v) formaldehyde in phosphate-buffered saline with 0.1% Tween-20 (PBST). Cells were rinsed three times in PBST for 5 minutes and then blocked for 1 hour with 10 mg/ml bovine serum albumin (BSA) in PBST. Cells were rinsed three times with PBST and incubated overnight (4°C) in primary antibody (see below) diluted in PBST followed by three more PBST rinses. Fluorescein (FITC)-conjugated AffiniPure Goat Anti-Rabbit IgG (Jackson ImmunoResearch) diluted 1:100 in PBST was added to visualise the primary antibody in combination with (1:50 dilution in PBST) Rhodamine-phalloidin (Molecular Probes) to visualise filamentous actin. Cells were incubated in labelling solution for at least 1 hour at 37°C or overnight at 4°C followed by PBST rinses. Vectashield (Vector Labs) was added to prevent photobleaching. Primary antibodies: rabbit polyclonal anti-RhoA IgG (Santa Cruz Biotechnology) diluted 1:100. Controls in which either the primary or secondary antibody was omitted revealed autofluorescence of yolk platelets in the cell body but no autofluorescence or non-specific antibody binding in growth cones. Cells were observed with a BioRad Microradiance laser-scanning confocal microscope using a 60×/1.3 NA water immersion objective on an Olympus microscope.

Fluorescence intensity plots

The relative intensity of anode/cathode RhoA immunofluorescence was quantified (Metamorph software, Universal Imaging) from greyscale images of growth cones double labelled with Rhodamine-phalloidin and an antibody to RhoA. The EF direction was horizontal in all images and intensity measurements were made from cathode- and anode-facing sides of growth cones within a single confocal image plane (at the level of the lamellipodium). This avoids regional intensity artefacts introduced by summing a z-series of confocal images in which one region of the growth cone spans more z-planes than another (for example, upon asymmetric collapse and rounding). The outline of the growth cone (including lamellipodia, but excluding filopodia) was traced onto the Rhodamine-phalloidin image plane, which reveals the entire growth cone. The outline was transferred to the Rho fluorescence image plane and was divided into anode- and cathode-facing regions by a line that describes the angle of the growth cone relative to the EF (e.g. Fig. 3C). The mean intensity of greyscale pixel values (from 0=black to 255=white) was calculated for each region (none contained areas of pixel saturation). Background subtraction was not performed since relative comparisons were made within single images and background values were uniform (Fig. 3F). Fluorescence symmetry was quantified as the ratio (average anode intensity/average cathode intensity) for each growth cone. A symmetrically fluorescent growth cone ratio=1 but if fluorescence was brighter anodally than cathodally the value would be >1, and if it was brighter cathodally than anodally the value would be <1. All growth cones were initially analysed (regardless of orientation relative to the EF) but subsequent analysis eliminated those facing the anode or cathode directly, leaving only those orthogonal to the EF direction (±45°). Mean ratios were compared using a two-tailed Student's *t* test.

Supported by The Wellcome Trust.

References

Aktories, K., Braun, U., Rosener, S., Just, I., and Hall, A. (1989). The rho gene product expressed in *E. coli* is a substrate of botulinum ADP-ribosyltransferase C3. *Biochem. Biophys. Res. Commun.* **158**, 209-213.

Bailey, N. T. J. (1981). *Statistical Methods in Biology* (2nd edn.), pp. 38-39. London: Hodder and Stoughton.

Brabeck, C., Beschorner, R., Conrad, S., Mittelbronn, M., Bekure, K., Meyermann, R., Schluesener, H. J., and Schwab, J. M. (2004). Lesional expression of RhoA and RhoB following traumatic brain injury in humans. *J. Neurotrauma* **21**, 697-706.

Campbell, D. S. and Holt, C. E. (2003). Apoptotic pathway and MAPKs differentially regulate chemotropic responses of retinal growth cones. *Neuron* **376**, 939-952.

Chaves-Olarte, E., Weidmann, M., Eichel-Streiber, C. and Thelestam, M. (1997). Toxins A and B from *Clostridium difficile* differ with respect to enzymatic potencies, cellular substrate specificities, and surface binding to cultured cells. *J. Clin. Invest.* **100**, 1734-1741.

Davies, S. P., Reddy, H., Caivano, M. and Cohen, P. (2000). Specificity and mechanism of action of some commonly used protein kinase inhibitors. *Biochem. J.* **351**, 95-105.

Di Cunto, F., Ferrara, L., Curtetti, R., Imaisio, S., Guazzone, S., Broccoli, V., Bulfone,

A., Altruda, F., Vercelli, A. and Sikengo, L. (2003). Role of citron kinase in dendritic morphogenesis of cortical neurons. *Brain Res. Bull.* **60**, 319-327.
Doussau, F., Gasman, S., Humeau, Y., Vitiello, F., Popoff, M., Boquet, P., Bader, M.-F. and Poulain, B. (2000). A rho-related GTPase is involved in Ca^{2+}-dependent neurotransmitter exocytosis. *J. Biol. Chem.* **275**, 7764-7770.
Duncia, J. V., Santella, J. B., III, Higley, C. A., Pitts, W. J., Wityak, J., Frietze, W. E., Rankin, F. W., Sun, J.-H., Earl, R. A., Tabaka, A. C. et al. (1998). MEK inhibitors: the chemistry and biological activity of U0126, its analogs, and cyclization products. *Bioorg. Med. Chem. Lett.* **8**, 2839-2844.
Dunican, D. J. and Doherty, P. (2001). Designing cell-permeant phosphopeptides to modulate intracellular signalling pathways. *Biopolymers* **60**, 45-60.
Erskine, L. and McCaig, C. D. (1995). Growth cone neurotransmitter activation modulates electric field guided nerve growth. *Dev. Biol.* **171**, 330-339.
Erskine, L., Stewart, R. and McCaig, C. D. (1995). Electric field-directed growth and branching of cultured frog nerves: effects of aminoglycosides and polycations. *J. Neurobiol.* **26**, 523-536.
Fournier, A. E., Takizawa, B. T. and Strittmatter, S. M. (2003). Rho kinase inhibition enhances axonal regeneration in the injured CNS. *J. Neurosci.* **23**, 1416-1423.
Fujisawa, K., Madaule, P., Ishizaki, T., Watanabe, G., Bito, H., Saito, Y., Hall, A. and Narumia, S. (1998). Different regions of Rho determine Rho-selective binding of different classes of Rho target molecules. *J. Biol. Chem.* **273**, 18943-18949.
Fukata, M., Watanabe, T., Noritake, J., Nakagawa, M., Yamaga, M., Iwamatsu, A., Perez, F. and Kaibuchi, K. (2002). Rac and cdc42 capture microtubules through IGGAP1 and CLIP-170. *Cell* **109**, 873-885.
Fukata, M., Nakagawa, M. and Kaibuchi, K. (2003). Roles of Rho-family GTPases in cell polarisation and directional migration. *Curr. Opin. Cell Biol.* **15**, 590-597.
Giniger, E. (2002). How do Rho family GTPases direct axon growth and guidance? A proposal relating signalling pathways to growth cone mechanics. *Differentiation* **70**, 385-396.
Gordon-Weeks, P. (2003). Microtubules and growth cone function. *J. Neurobiol.* **58**, 70-83.
Henley, J. and Poo, M.-M. (2004). Guiding neuronal growth cones using Ca^{2+} signals. *Trends Cell Biol.* **14**, 320-330.
Herrmann, C., Wray, J., Travers, F. and Barman, T. (1992). Effect of 2,3-butanedione monoxime on myosin and myofibrillar ATPases. An example of an uncompetitive inhibitor. *Biochemistry* **31**, 12227-12232.
Hinkle, L., McCaig, C. D. and Robinson, K. R. (1981). The direction of growth of differentiating neurons and myoblasts from frog embryos in an applied electric field. *J. Physiol.* **314**, 121-135.
Hotary, K. B. and Robinson, K. R. (1991). The neural tube of the *Xenopus* embryo maintains a potential difference across itself. *Dev. Brain Res.* **59**, 65-73.
Hotary, K. B. and Robinson, K. R. (1992). Evidence for a role for endogenous electrical fields in chick embryo development. *Development* **114**, 985-996.
Hotary, K. B. and Robinson, K. R. (1994). Endogenous electrical currents and voltage gradients in *Xenopus* embryos and the consequences of their disruption. *Dev. Biol.* **166**, 789-800.
Howe, A. K. (2004). Regulation of actin-based cell migration by cAMP/PKA. *Biochim. Biophys. Acta* **1692**, 159-174.
Jin, M., Guan, C.-B., Jiang, Y.-A., Chen, G., Zhao, C.-T., Cui, K., Song, Y.-Y, Wu, C.-P., Poo, M.-M. and Yuan, X.-B. (2005). Ca^{2+}-dependent regulation of Rho GTPases triggers turning of nerve growth cones. *J. Neurosci.* **25**, 2338-2347.
Kaibuchi, K., Kuroda, S. and Amano, M. (1999). Regulation of the cytoskeleton and cell adhesion by the rho family GTPases in mammalian cells. *Annu. Rev. Biochem.* **68**, 459-486.
Kaufmann, N., Wills, Z. P. and Van Vactor, D. (1998). *Drosophila* Rac1 controls motor axon guidance. *Development* **125**, 453-461.
Kim, M. D., Kolodziej, P. and Chiba, A. (2002). Growth cone pathfinding and filopodial dynamics are mediated separately by cdc42 activation. *J. Neurosci.* **22**, 1794-1806.
Kozma, R., Sarner, S., Ahmed, S. and Lim, L. (1997). Rho family GTPases and neuronal growth cone remodelling: relationship between increased complexity induced by Cdc42Hs, Rac1, and acetylcholine and collapse induced by RhoA and lysophosphatidic acid. *Mol. Cell. Biol.* **17**, 1201-1211.
Kranenburg, O., Poland, M., van Horck, F. P. G., Drechsel, D., Hall, A. and Moolenaar, W. H. (1999). Activation of rhoA by lysophosphatidic acid and $G\alpha_{12/13}$ subunits in neuronal cells: induction of neurite retraction. *Mol. Biol. Cell* **10**, 1851-1857.
Lee, H., Engel, U., Rusch, J., Scherrer, S., Sheard, K. and Van Vactor, D. (2004). The microtubule plus end tracking protein Orbit/MAST/CLASP acts downstream of the tyrosine kinase Abl in mediating axon guidance. *Neuron* **42**, 913-926.
Li, Y., Jia, Y.-C., Cui, K., Li, N., Zheng, Z.-Y., Wang, Y.-Z. and Yuan, X.-B. (2005). Essential role of TRP channels in the guidance of nerve growth cones by brain derived neurotrophic factor. *Nature* **434**, 894-898.
Madura, T., Yamashita, T., Kubo, T., Fujitani, M., Hosokawa, K. and Tohyama M. (2004). Activation of Rho in the injured axons following spinal cord injury. *EMBO Rep.* **5**, 412-417.
McCaig, C. D. (1987). Spinal neurite reabsorption and regrowth in vitro depend on the polarity of an applied electric field. *Development* **100**, 31-41.
McCaig, C. D., Sangster, L. and Stewart, R. (2000). Neurotrophins enhance electric field-directed growth cone guidance and directed nerve branching. *Dev. Dyn.* **217**, 299-308.
McCaig, C. D., Rajnicek, A. M., Song, B. and Zhao, M. (2002). Has electrical growth cone guidance found its potential? *Trends Neurosci.* **25**, 354-358.
McCaig, C. D., Rajnicek, A. M., Song, B. and Zhao, M. (2005). Controlling cell behavior electrically: current views and future potential. *Physiol. Rev.* **85**, 943-978.
Metcalf, M. E. M. and Borgens, R. B. (1994). Weak applied voltages interfere with amphibian morphogenesis and pattern. *J. Exp. Zool.* **268**, 322-338.
Ming, G. L., Wong, S. T., Henley, J., Yuan, X. B., Song, H. J., Spitzer, N. C. and Poo, M. M. (2002). Adaptation in the chemotactic guidance of nerve growth cones. *Nature* **417**, 411-418.
Mueller, B. K. (1999). Growth cone guidance: first steps to a deeper understanding. *Annu. Rev. Neurosci.* **22**, 351-388.
Narumiya, S., Morii, N., Sekine, A. and Kozaki, S. (1990). ADP-ribosylation of the rho/rac gene products by botulinum ADP-ribosyltransferase: identity of the enzyme and effects on protein and cell functions. *J. Physiol. (Paris)* **84**, 267-272.
Nieuwkoop, P. D. and Faber, J. (1956). *Normal Table of Xenopus laevis (Daudin).* Amsterdam: North Holland.
Orida, N. and Poo, M. M. (1978). Electrophoretic movement and localisation of acetylcholine receptors in the embryonic muscle cell membrane. *Nature* **275**, 31-35.
Palmer, A. M., Messerli, M. A. and Robinson, K. R. (2000). Neuronal galvanotropism is independent of external Ca^{2+} entry or internal Ca^{2+} gradients. *J. Neurobiol.* **45**, 30-38.
Patel, B. N. and Van Vactor, D. L (2002). Axon guidance: they cytoplasmic tail. *Curr. Opin. Cell Biol.* **14**, 221-229.
Patel, N. and Poo, M. M. (1982). Orientation of neurite growth by extracellular electric fields. *J. Neurosci.* **2**, 483-496.
Raftopoulou, M. and Hall, A. (2004). Cell migration: rho GTPases lead the way. *Dev. Biol.* **265**, 23-32.
Rajnicek, A. M., Robinson, K. R. and McCaig, C. D. (1998). The direction of neurite growth in a weak DC electric field depends on the substratum: contributions of adhesivity and net surface charge. *Dev. Biol.* **203**, 412-423.
Rajnicek, A. M., Foubister, L. E. and McCaig, C. D. (2006). Growth cone steering by a physiological electric field requires dynamic microtubules, microfilaments and Rac-mediated filopodial asymmetry. *J. Cell Sci.* **119**, 1736-1745.
Ruchhoeft, M. L. and Harris, W. A. (1997). Myosin functions in *Xenopus* retinal ganglion cell growth cone motility in vivo. *J. Neurobiol.* **32**, 567-578.
Servant, G., Weiner, O. D., Herzmark, P., Balla, T., Sedat, J. W. and Bourne, H. R. (2004). Polarization of chemoattractant receptor signalling during neutrophil chemotaxis. *Science* **287**, 1037-1040.
Shapiro, S., Borgens, R., Pascuzzi, R., Roos, K., Groff, M., Purvines, S., Rodgers, R. B., Hagy, S. and Nelson, P. (2005). Oscillating field stimulation for complete spinal cord injury in humans: a phase 1 trial. *J. Neurosurg. Spine* **2**, 3-10.
Shi, R. and Borgens, R. B. (1994). Embryonic neuroepithelium sodium transport, the resulting physiological potential and cranial development. *Dev. Biol.* **165**, 105-116.
Shi, R. and Borgens, R. B. (1995). Three dimensional gradients of voltage during development of the nervous system as invisible coordinates for the establishment of the embryonic pattern. *Dev. Dyn.* **202**, 101-114.
Song, B., Zhao, M., Forrester, J. and McCaig, C. (2004). Nerve regeneration and wound healing are stimulated and directed by an endogenous electrical field in vivo. *J. Cell Sci.* **117**, 4681-4690.
Song, H. and Poo, M.-M. (2001). The cell biology of neuronal navigation. *Nat. Cell Biol.* **3**, E81-E88.
Song, H.-J., Ming, G.-l. and Poo, M.-M. (1997). cAMP-induced switching in turning direction of nerve growth cones. *Nature* **388**, 275-279.
Sta Iglesia, D. D. and Vanable, J. W., Jr (1998). Endogenous lateral electric fields around bovine corneal lesions are necessary for and can enhance normal rates of wound healing. *Wound Repair Regen.* **6**, 531-542.
Stewart, R., Erskine, L. and McCaig, C. D. (1995). Calcium channel subtypes and intracellular calcium stores modulate electric field-stimulated and -oriented nerve growth. *Dev. Biol.* **171**, 340-351.
Sung, J.-K., Miao, L., Calvert, J. W., Huang, L., Harkey, H. L. and Zhang, J. H. (2003). A possible role of RhoA/Rho-kinase in experimental spinal cord injury in rat. *Brain Res.* **959**, 29-38.
Taniguchi, T., Kawamata, T., Mukai, H., Hasegawa, H., Isagawa, T., Yasuda, M., Hashimoto, T., Terashima, A., Nakai, M., Mori, H. et al. (2001). Phosphorlylation of tau is regulated by PKN. *J. Biol. Chem.* **276**, 10025-10031.
Thies, E. and Davenport, R. W. (2002). Independent roles of rho-GTPases in growth cone and axonal behavior. *J. Neurobiol.* **54**, 358-369.
Uehata, M., Ishizaki, T., Satoh, H., Ono, T., Kawahara, T., Morishita, T., Tamakawa, H., Yamagami, K., Inui, J., Maekawa, M. et al. (1997). Calcium sensitization of smooth muscle mediated by a Rho-associated protein kinase in hypertension. *Nature* **389**, 990-994.
Vastrik, I., Eickholt, B. J., Walsh, F. S., Ridley, A. and Doherty, P. (1999). Sema-3 induced growth cone collapse is mediated by Rac 1 amino acids 17-32. *Curr. Biol.* **9**, 991-998.
Vlahos, C. J., Matter, W. F., Hui, K. Y. and Brown, R. F. (1994). A specific inhibitor of phosphatidylinositol 3-kinase, 2-(4-morpholinyl)-8-phenyl-4H-1-benzopyran-4-one (LY294002). *J. Biol. Chem.* **269**, 5241-5248.
Wahl, S., Barth, H., Ciossek, T., Aktories, K. and Mueller, B. K. (2000). Ephrin-A5 induces collapse of growth cones by activating Rho and Rho kinase. *J. Cell Biol.* **149**, 263-270.
Wang, E., Zhao, M., Forrester, J. V. and McCaig, C. D. (2003). Electric fields and MAP kinase signaling can regulate early wound healing in lens epithelium. *Invest. Ophthalmol. Vis. Sci.* **44**, 244-249.
Wen, Z., Guirland, C., Min, G.-l. and Zheng, J. Q. (2004). A CaMKII/calcineurin switch controls the direction of Ca^{2+}-dependent growth cone guidance. *Neuron* **43**, 835-846.

Journal of Cell Science

Yamada, T., Ohoka, Y., Kogo, M. and Inagaki, S. (2005). Physical and functional interactions of the lysophosphatidic acid receptors with PDZ domain-containing rho guanine nucleotide exchange factors (RhoGEFs). *J. Biol. Chem.* **280**, 19358-19363.

Yamamoto, N., Tamada, A. and Murakami, F. (2003). Wiring of the brain by a range of guidance cues. *Prog. Neurobiol.* **68**, 393-407.

Yuan, X. B., Jin, M., Xu, X., Song, Y. Q., Wu, C. P., Poo, M. M. and Duan, S. (2003). Signalling and crosstalk of Rho GTPases in mediating axon guidance. *Nat. Cell Biol.* **5**, 38-45.

Zhao, M., Pu, J., Forrester, J. V. and McCaig, C. D. (2002). Membrane lipids, EGF receptors, and intracellular signals colocalize and are polarized in epithelial cells moving directionally in a physiological electric field. *FASEB J.* **16**, 857-859.

Journal of Cell Science